DOI: 10.33184/bulletin-bsu-2023.3.2

3D MODEL OF PLASMA PROCESSES IN RADIO FREQUENCY INDUCTIVELY COUPLED PLASMA TORCH OF 30 KW, 5.28 MHZ FOR POWDER TREATMENT

© D. V. Ivanov*, S. G. Zverev

Peter the Great St. Petersburg Polytechnic University
29 Polytechnicheskaya Street, 195251 St. Petersburg, Russia.

**Email: d.ivanov@spbstu.ru*

The paper presents a 3D stationary model of plasma processes in the radio frequency inductively coupled plasma torch of 30 kW, 5.28 MHz for powder treatment and shows the results of calculations for various flow rates of the plasma-forming gas (air). A short review of existing models has been made. The basic equations of the model are presented. The geometry of the studied plasma torch is shown. The calculation results are presented in the form of plasma temperature and axial velocity distributions in two mutually perpendicular sections. The distributed results of calculations made it possible to obtain integral parameters of the plasma torch, such as the plasma jet power, torch wall power losses, and radiation power losses. The analysis of the received results is carried out.

The use of a three-dimensional model made it possible to observe the features of the plasma temperature and velocity distributions that could not be seen within the framework of a two-dimensional axisymmetric model. It can be seen that the plasma is tilted in relation to the axis of the plasma torch. This effect is observed in a cross-section perpendicular to the direction of the inductor ends. This phenomenon can be explained by the spiral shape of the inductor, in which the axisymmetric shape of the electromagnetic field is disturbed.

***Keywords**: inductively coupled plasma, radio frequency torch, fine powder treatment, mathematical simulation, 3D model.*

Introduction

Currently, radio frequency (RF) inductively coupled plasma (ICP) torches are used for such technologies as spectral analysis, purification and spheroidization of fine powders, surface treatment, nanopowders production, plasma-chemical technologies [1–6]. In most cases, plasma is generated in the plasma torch, and then a plasma jet flows into the plasma reactor, where the necessary treatment takes place. The shape of the plasma temperature and velocity distributions at the plasma torch outlet section can vary depending on the design of the plasma torch and the mode of its operation [7–9], which has a great influence on the processes in the plasma reactor.

The review of papers devoted to simulation of RF ICP torches is given in the book [3]. In recent years, researchers have developed a large number of new models of processes in RF ICP torches that have shown good agreement with experimental data [7–19]. These models depending on the goal differ in the space dimension (2D or 3D), the assumption of plasma equilibrium (LTE models, or 2T models, or models with chemical non-equilibrium), the assumption of plasma laminarity (laminar models or different turbulent models), and other.

The axial symmetry condition is usually used in 2D models, which makes it possible to obtain plasma temperature and velocity distributions in two coordinates (r, z) of a cylindrical coordinate system. The disadvantages of such models include overestimation of the tangential velocity in the case of swirling gas feeding and difficulties of the calculation convergence at high gas flow rates [9].

3D models of RF ICP torches appeared not so long ago; their development was limited by the level of computational resources. Significant achievements in this field were reached by a scientific group of V. Colombo and others (Italy). Features of its model and the main results were published in papers [10–15] and other. Calculations were carried in the ANSYS Fluent software using the technology UDF (user-defined functions written in C++). The computational mesh consists of tetrahedrons and hexahedrons. Approximate number of cells of the grid is $4.5 \cdot 10^5$ (varies slightly depending on the configuration of the plasma torch and inductor coils). Modeling was performed on a cluster of workstations. The results of calculations for ICP torches with different geometry of inductor coils shown in [10–15] suggest that the geometry of the inductor coils has a significant influence on the distribution of plasma parameters in ICP torches. Depending on the geometry of the inductor coils a disturbance of axial symmetry of the plasma parameters can be either insignificant or significant.

RF plasma is widely used for purification and spheroidization of fine powder that is fed to the output of the RF plasma torch [20–23]. Knowledge of the 3D features of the plasma temperature and velocity distributions in the outlet section of the plasma torch will make it possible to feed the powder more rationally into the plasma jet and to increase the productivity of the process.

In this article, results of simulation using a three-dimensional model of the processes in the RF ICP torch for fine powder treatment are presented. A photo of the studied plasma torch is shown in *Fig.* 1, where the outlet of the torch is located on the left, the plasma jet flows into the plasma reactor (the reactor not shown).

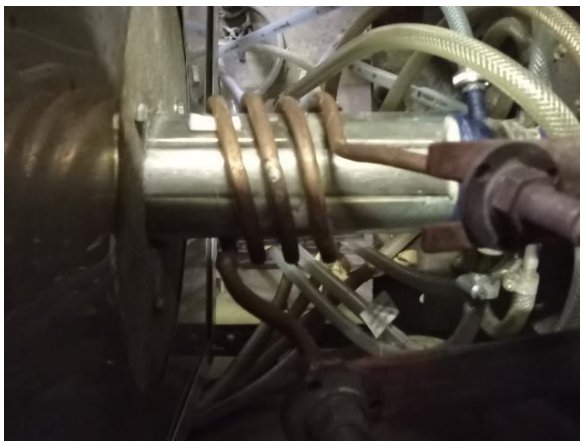

Fig. 1. Photo of the studied ICP torch.

Mathematical model

The basic equations of the used model of plasma processes (it is assumed that plasma is in the state of local thermodynamic equilibrium) express the fundamental conservation laws (of energy, momentum and mass), and for the elementary volume are written as follows [7]:

- energy equation:

$$\nabla \cdot (\rho \vec{v} H) = \sigma E^2 - u_{rad} + \nabla \cdot \left(\frac{\lambda}{c_p} \nabla H \right); \quad (1)$$

- motion equation:

$$\nabla \cdot (\rho \vec{v} \vec{v}) = -\nabla p + \overrightarrow{F_B} + \rho \vec{g} + \nabla \cdot (\mu \nabla \vec{v}); \quad (2)$$

- continuity equation:

$$\nabla \cdot (\rho \vec{v}) = 0. \quad (3)$$

Equations *(1)–(3)* include:

- plasma parameters such as enthalpy H that related to temperature T; velocity $\vec{v}$; pressure p;
- thermophysical plasma properties such as density ρ; thermal conductivity λ; specific heat c_p; viscosity μ; electrical conductivity σ; specific radiation power u_{rad};
- electromagnetic values such as electric field intensity E; electromagnetic force $\overrightarrow{F_B} = \vec{J} \times \vec{B}$.

Since plasma exists in an electromagnetic field, the system of equations (1)–(3) is supplemented by Maxwell's system of electromagnetic equations:

$$\begin{cases} \nabla \times \vec{E} = -\dfrac{\partial \vec{B}}{\partial t}, & \nabla \cdot \vec{E} = \dfrac{\rho_{el}}{\varepsilon_0}, \\ \nabla \times \vec{H} = \vec{J}, & \nabla \cdot \vec{B} = 0, \end{cases}$$

where $\vec{E}$ and $\vec{H}$ are electric and magnetic field intensities; $\vec{B}$ is magnetic induction; $\vec{J}$ is current density; ρ_{el} is volume density of electrical charge; ε_0 is electric constant.

For thermal plasma processes, the Maxwell's system of equations is reduced to equation for the vector potential $\vec{A}$:

$$\Delta \vec{A} - \varepsilon_0 \mu_0 \frac{\partial^2 \vec{A}}{\partial t^2} = -\mu_0 \vec{J}, \quad (4)$$

where $\vec{J} = \sigma \vec{E}$, $\vec{B} = \nabla \times \vec{A}$.

Thus, equations *(1)–(4)* represent a system of equations that need to be solved simultaneously to obtain the distributions of the required plasma parameters, namely, temperature, velocity, pressure, electromagnetic quantities.

To take into account radiation heat transfer, the model of optically thin plasma was used. The dependences of specific radiation power u_{rad} on temperature, as well as the dependences of thermodynamic and transport properties of air plasma, were taken from the books [24–25].

A plasma turbulence was taken into account using the SST-model, which is a combination of the k-ε and k-ω turbulence models: equations of the k-ε model are used to calculate the flow in a free area, and equations of the k-ω model – in the near-wall area.

The boundary conditions of the used model are described in detail in [7]. The developed model showed good agreement with the experimental data presented in the book [1].

In the model it is assumed that the coil current is uniformly distributed over the coil cross section.

Data for calculation

The ICP/RF plasma torch with the following main dimensions is considered (see *Fig.* 2): the torch length is $L_0 = 270$ mm, the internal diameter of the discharge chamber is $D_0 = 54$ mm, the internal diameter of the inductor coils is $D_1 = 92$ mm, the external diameter of the torch tube is $D_2 = 70$ mm, the external diameter of the internal tube is $D_3 = 48$ mm (the gas is fed axially into a gap between the internal and external tubes), the height of the inductor coils is $h = 70$ mm, the number of coils is 4, the diameter of the coil conductor tube is $d = 10$ mm, the distance from the torch inlet to the inductor is $L_1 = 140$ mm.

As seen from *Fig.* 1, the studied plasma torch is a device with a copper split water-cooled chamber covered by a quartz tube. This feature was not taken into account in the simulation, it was assumed that the discharge chamber is a thick-walled quartz tube (see *Fig.* 3), and the temperature of 300 K is set on its inner surface.

To take into account the electromagnetic field around the inductor coils, the computational domain was chosen in the shape of a cylinder with a diameter of 400 mm, inside of which the plasma torch is situated.

The task was solved as a three-dimensional case using ANSYS Fluent software. A tetrahedral mesh was used at the simulation: ~2.6 million cells in the plasma region, ~ 6.5 million cells in the surrounding space.

The operating parameters of the plasma torch: the current frequency $f = 5.28$ MHz, plasma power is $P_{pl} = 30$ kW, pressure at the outlet of the plasma torch is $p = 1$ atm, plasma gas is air, plasma gas flow rates: $G = 40, 80, 120$ slpm.

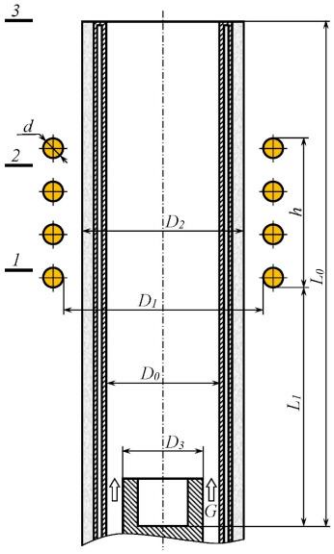

Fig. 2. Design of the studied ICP torch.

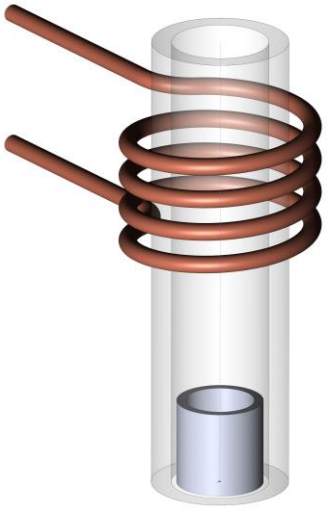

Fig. 3. The ICP torch geometry used in simulations.

Results and discussion

Plasma temperature and axial velocity distributions in the different cross-sections of the torch are shown in *Figs.* 4–6. The locations of the cross-sections $z_1 = 150$ mm, $z_2 = 200$ mm, $z_3 = 270$ mm (for which the temperature distributions are shown in *Figs*. 4–6) can be seen on the left side of *Fig*. 2. The distributed results of calculations made it possible to obtain integral parameters of the plasma torch that are presented in *Table* 1.

Analysis of the results shows that:

1. The use of a three-dimensional model made it possible to observe the features of the plasma temperature distributions that could not be seen within the framework of a two-dimensional axisymmetric model. It can be seen that the plasma is tilted in relation to the axis of the plasma torch. This effect is observed in a cross-section perpendicular to the direction of the inductor ends (see *Fig.* 4–6, b). This phenomenon can be explained by the spiral shape of the inductor, in which the axisymmetric shape of the electromagnetic field is disturbed. The fact is that an electromagnetic force acts on the plasma, directed to the axis of the plasma torch. But in the central (in height) region of the inductor, this force acts from all sides of the torch wall, compressing the plasma. However, in the lower part of the inductor, this force acts on the left (see *Fig.* 4–6, b) and is not compensated on the right, since the lower turn does not continue to the right side, it goes to the inductor end. In the upper part of the inductor, on the contrary, the force acts on the left and is not compensated on the right. Under the action of this force the axis of the plasma is tilted with respect to the axis of the plasma torch.

2. An increase in the gas flow rate leads to a decrease in the plasma diameter. It can be explained as follows: the RF plasma operates like an electromagnetic pump, i.e. only part of the gas flow fed into the torch participates in the plasma formation [1]. This quantity of gas is determined by the electromagnetic force, which depends on the coil current (and hence on the dissipated power). The part of gas which is not carried into the central part of the plasma torch by electromagnetic force moves along the torch walls.

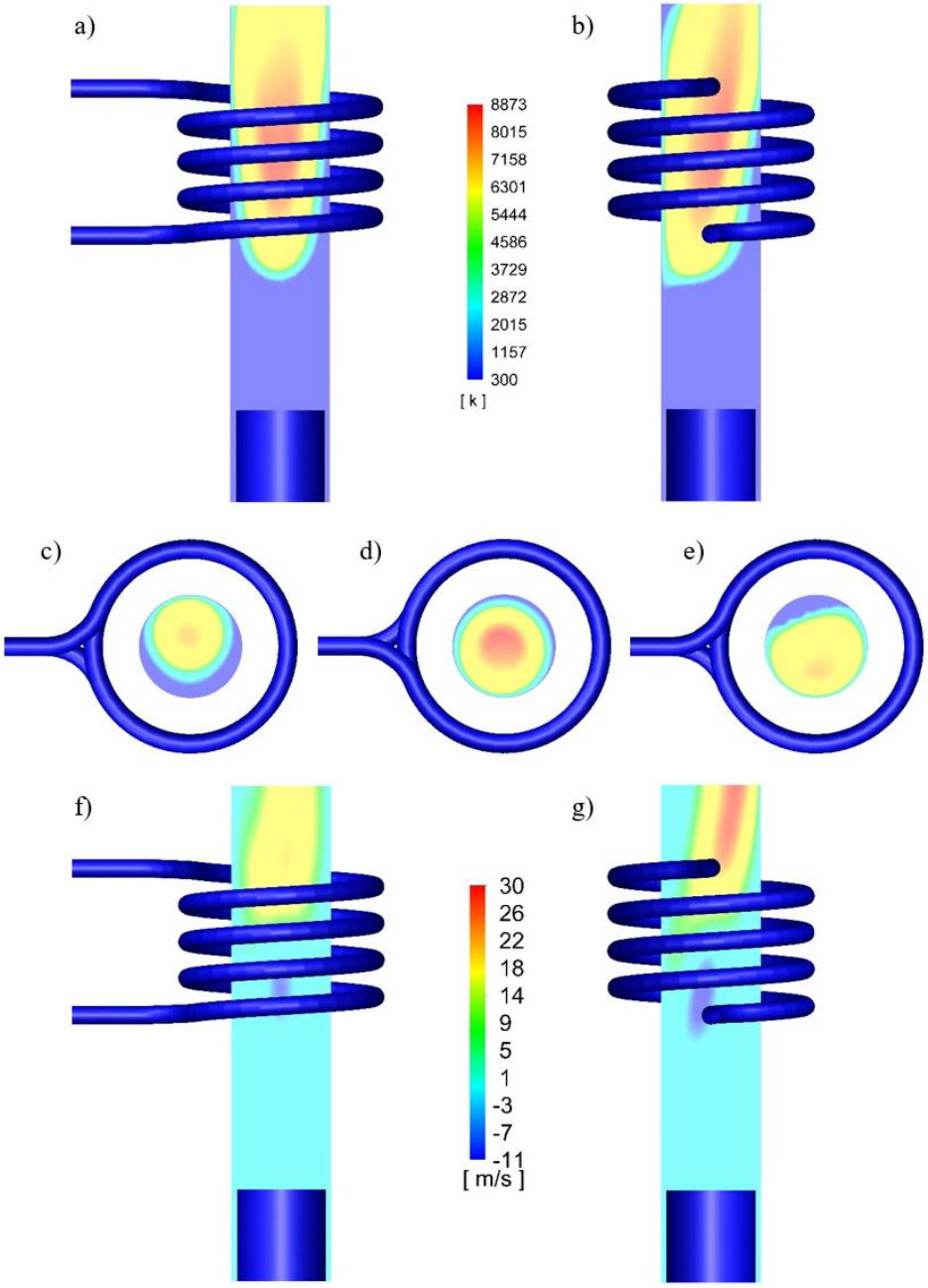

Fig. 4. Results of calculation at the gas flow rate G = 40 slpm: a, b – temperature distributions in two mutually perpendicular cross-sections; c–e – temperature distributions in cross-sections perpendicular to the plasma torch axis (c – z_1 = 150 mm, d – z_2 = 200 mm, e – z_3 = 270 mm); f, g – distributions of axial velocity in two mutually perpendicular cross-sections.

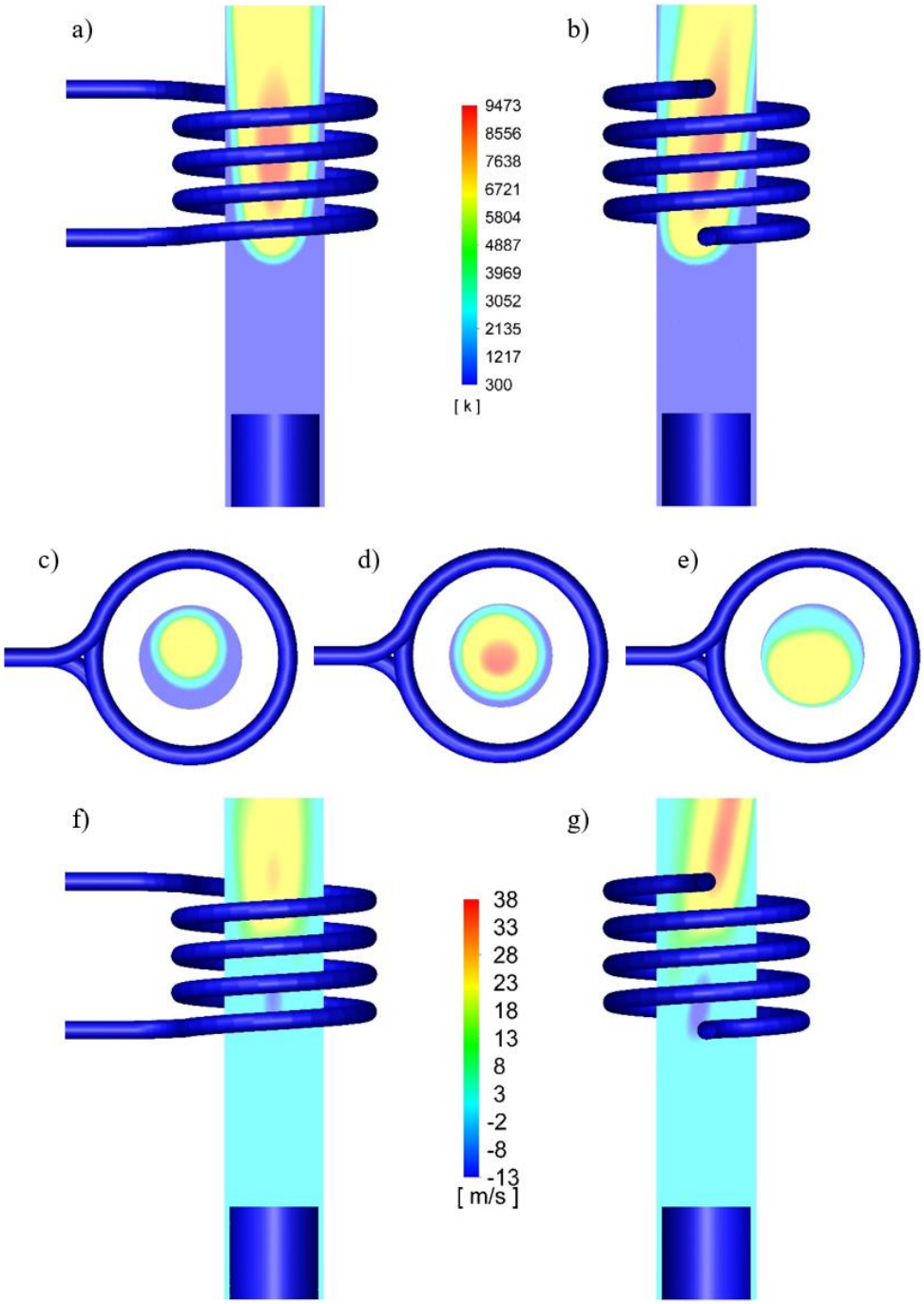

Fig. 5. Results of calculation at the gas flow rate G = 80 slpm: a, b – temperature distributions in two mutually perpendicular cross-sections; c–e – temperature distributions in cross-sections perpendicular to the plasma torch axis (c – z_1 = 150 mm, d – z_2 = 200 mm, e – z_3 = 270 mm); f, g – distributions of axial velocity in two mutually perpendicular cross-sections.

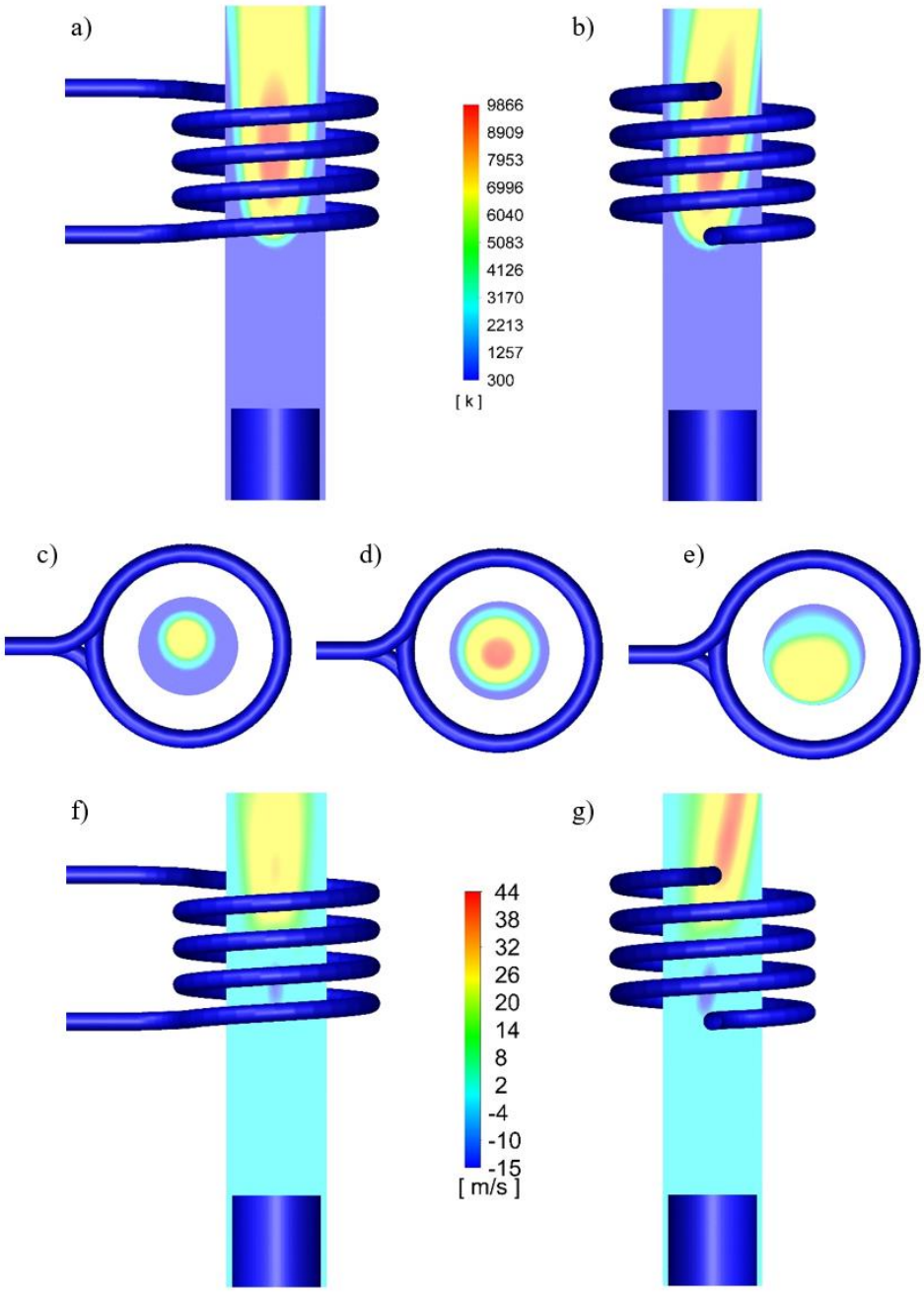

Fig. 6. Results of calculation at the gas flow rate G = 120 slpm: a, b – temperature distributions in two mutually perpendicular cross-sections; c-e – temperature distributions in cross-sections perpendicular to the plasma torch axis (c – z_1 = 150 mm, d – z_2 = 200 mm, e – z_3 = 270 mm); f, g – distributions of axial velocity in two mutually perpendicular cross-sections.

As the flow rate increases, more and more of the cold gas flows along the wall, which leads to a decrease in the temperature of the near-wall region of the plasma torch.

3. An increase in the gas flow rate from 40 to 120 slpm leads to an increase in temperature (from 8 873 K to 9 866 K, see *Table* 1) and also to an increase in the axial velocity of the plasma, both in the forward direction (towards the outlet) and in the opposite direction.

This is explained by the fact that an increase in the gas flow rate leads to a decrease in the plasma diameter, i.e. to a decrease in the electromagnetic coupling of the plasma with the inductor. Therefore, to maintain the plasma power at a level of 30 kW, the inductor current increases: 40 slpm corresponds to 152 A, 80 slpm – 178 A, 120 slpm – 207 A (see *Table* 1). Accordingly, an increase in the inductor current leads to an increase in the electromagnetic force acting on the plasma, which leads to an increase in plasma velocity.

4. Increasing of the gas flow rate from 40 to 80 slpm leads to a significant decrease in power losses in the torch wall – from 27.53% to 8.279% (percentages are taken from the power dissipated in the plasma), which is explained by the gas

thermal protection of the walls [1]. A further increase in the gas flow rate from 80 to 120 slpm leads to a further decrease in wall losses to 3.755%. Accordingly, a decrease in the power of losses to the wall leads to an increase in the power of the plasma jet (see *Table* 1), and hence to an increase in the efficiency of the plasma process.

5. The power losses due to plasma radiation are not high and increase insignificantly with increasing of the gas flow rate – from 3.952% at G = 40 l/min to 5.234% at G = 120 l/min (see *Table* 1).

Table 1

Integral results of calculations

Parameter	Symbol	Unit	Gas flow rate, slpm		
			40	80	120
Plasma power	P_{pl}	kW	30 (100%)	30 (100%)	30 (100%)
Coil current	I	A	152	178	207
Radiation power losses	P_{rad}	kW	1.186 (3.952%)	1.261 (4.200%)	1.570 (5.234%)
Torch wall power losses	P_{wall}	kW	8.259 (27.53%)	2.487 (8.279%)	1.127 (3.755%)
Power at the torch outlet (power of plasma jet)	P_{jet}	kW	19.694 (65.64%)	25.046 (83.39%)	27.343 (91.13%)
Calculation error	P_{error}	kW	0.863 (2.877%)	1.241 (4.133%)	–0.036 (0.121%)
Maximal temperature	T_{max}	K	8873	9473	9866

Conclusions

1. The distributions of plasma temperature and velocity in the direct-jet ICP/RF plasma torch with a power of 30 kW and gas flow rate up to 120 slpm was obtained.

2. The use of a three-dimensional model made it possible to observe that the plasma is tilted in relation to the axis of the plasma torch.

3. An increase in the gas flow rate from 40 to 120 slpm leads to an increase in temperature (from 8873 K to 9866 K), as well as in the axial velocity of the plasma, and leads to a decrease in plasma diameter.

4. Increasing of the gas flow rate leads to a significant decrease in power losses in the torch wall, which is explained by the gas thermal protection of the walls.

5. Developed 3D model of plasma processes in the radio frequency inductively coupled plasma torch is a promising tool for studying existing plasma processes and creating new ones. Studies on this topic will continue.

The research was carried out within the framework of the research topic under the state assignment of Ministry of Science and Higher Education of the Russian Federation FSEG-2023-0012.

REFERENCES

1. Dresvin S. V., Donskoy A. V., Goldfarb V. M., Klubnikin V. S. Physics and technology of low-temperature plasmas. Iowa State Univ. Press. 1977. 471 p.
2. Дресвин С. В., Зверев С. Г. Плазмотроны: конструкции, параметры, технологии [Dresvin S. V., Zverev S. G. Plasma torches: designs, parameters, technologies]. СПб.: изд-во Политех. ун-та. 2007. 207 с.
3. Dresvin S., Zverev S., Ivanov D., Matveev I. High Frequency Induction Plasma Torches // Plasma Assisted Combustion, Gasification, and Pollution Control. Vol. 1. Methods of plasma generation for PAC. Outskirts Press, Inc. 2013. Pp. 373–462.
4. Matveev I. B., Zverev S. G., Matveyeva S. A. Progress in the second generation RF plasma development // Plasma Assisted Combustion, Gasification, and Pollution Control. Vol. 2. Combustion and Gasification. Outskirts Press, Inc. 2015. Pp. 450–455.
5. Adamovich I. et al. The 2017 Plasma Roadmap: Low temperature plasma science and technology. J. Phys. D. Appl. Phys. 2017. Vol. 50(32), 323001. DOI: 10.1088/1361-6463/aa76f5.
6. Boulos M. I., Fauchais P. L., Pfender E. Handbook of Thermal Plasmas. Springer International Publishing. 2023. 1975 p. DOI: 10.1007/978-3-030-84936-8.
7. Ivanov D. V., Zverev S. G. Mathematical Simulation of Processes in ICP/RF Plasma Torch for Plasma Chemical Reactions. IEEE Trans. Plasma Sci. 2017. Vol. 45(12). Pp. 3125–3129. DOI: 10.1109/TPS.2017.2773140.
8. Ivanov D. V, Zverev S. G. Mathematical Simulation of Processes in Air ICP/RF Plasma Torch for High-Power Applications. IEEE Trans. Plasma Sci. 2020. Vol. 48(2). Pp. 338–342. DOI: 10.1109/TPS.2019.2957676.
9. Ivanov D. V., Zverev S. G. Mathematical Simulation of Plasma Processes in a Radio Frequency Inductively Coupled Plasma Torch in ANSYS Fluent and COMSOL Multiphysics Software Packages. IEEE Trans. Plasma Sci. 2022. Vol. 50(6). Pp. 1700–1709. DOI: 10.1109/TPS.2022.3175741.
10. Abeele D. V., Degrez G. Efficient Computational Model for Inductive Plasma Flows. AIAA Journal. 2000. Vol. 38(2). Pp. 234–242. DOI: 10.2514/2.977.
11. Bernardi D., Colombo V., Ghedini E., Mentrelli A. Three-dimensional modelling of inductively coupled plasma torches. Eur. Phys. J. D. 2003. Vol. 22(1). Pp. 119–125. DOI: 10.1140/epjd/e2002-00233-9.
12. Bernardi D., Colombo V., Ghedini E., Mentrelli A. Three-dimensional effects in the modelling of ICPTs. Eur. Phys. J. D. 2003. Vol. 25(3). Pp. 271–277. DOI: 10.1140/epjd/e2003-00244-0.
13. Bernardi D., Colombo V., Ghedini E., Mentrelli A. Comparison of different techniques for the FLUENT©-based treatment of the electromagnetic field in inductively coupled plasma torches. Eur. Phys. J. D. 2003. Vol. 27(1). Pp. 55–72. DOI: 10.1140/epjd/e2003-00227-1.
14. Bernardi D., Colombo V., Ghedini E., Mentrelli A., Trombetti T. 3-D numerical simulation of fully-coupled particle heating in ICPTs. Eur. Phys. J. D. 2004. Vol. 28. Pp. 423–433. DOI: 10.1140/epjd/e2004-00012-8.
15. Colombo V., Ghedini E., Sanibondi P. Three-dimensional investigation of particle treatment in an RF thermal plasma with reaction chamber. Plasma Sources Sci. Technol. 2010. Vol. 19, 065024. DOI: 10.1088/0963-0252/19/6/065024.
16. Tanaka Y. Two-temperature chemically non-equilibrium modelling of high-power Ar–N2inductively coupled plasmas at atmospheric pressure. J. Phys. D. Appl. Phys. 2004. Vol. 37(8). Pp. 1190–1205. DOI: 10.1088/0022-3727/37/8/007.

17. Siregar Y., Tanaka Y., Ishijima T., Uesugi Y. Influence of sheath gas flow rate in Ar induction thermal plasma with Ti powder injection on the plasma temperature by numerical calculation. MATEC Web Conf. 2018. Vol. 218, 04030. DOI: 10.1051/matecconf/201821804030.
18. Shigeta M. Time-dependent 3D simulation of an argon RF inductively coupled thermal plasma. Plasma Sources Sci. Technol. 2012. Vol. 21(5). 55029. DOI: 10.1088/0963-0252/21/5/055029.
19. Shigeta M. Three-dimensional flow dynamics of an argon RF plasma with dc jet assistance: a numerical study. J. Phys. D. Appl. Phys. 2012. Vol. 46(1), 15401. DOI: 10.1088/0022-3727/46/1/015401.
20. Magnaval S., Morvan D., Amouroux J. et al. Treatment of metallurgical silicon powder by thermal RF plasma. High Temperature Material Processes. 1999. Vol. 3(4). Pp. 355–373.
21. Morvan D., Soric A., Benmansour M., Darwiche S., Francke E., Nikravech M., Amouroux J., Dresvin S. Hydrogenation and purification of silicon by RF plasma. High Temperature Material Processes. 2005. Vol. 9(3). Pp. 375–390. DOI: 10.1615/HighTempMatProc.v9.i3.50.
22. Amouroux J., Dresvin S., Zverev S. Investigation of a dusty RF plasma torch jet. High Temperature Material Processes. 2007. Vol. 11(1). Pp. 95–102. DOI: 10.1615/HighTempMatProc.v11.i1.80.
23. Дресвин С. В., Зверев С. Г. Теплообмен в плазме [Dresvin S. V., Zverev S. G. Heat transfer in plasma]. СПб.: изд-во Политех. ун-та. 2008. 212 с. DOI: 10.18720/SPBPU/2/si20-1009.
24. Энгельшт В. С., Гурович В. Ц., Десятков Г. А. и др. Низкотемпературная плазма. Т. 1. Теория столба электрической дуги [Engelsht V. S., Gurovich V. C., Desyatkov G. A. et al. The theory of the electric arc column. Vol. 1 Low temperature plasma]. Новосибирск: Наука. 1990. 376 с.
25. Дресвин С. В., Иванов Д. В. Физика плазмы [Dresvin S. V., Ivanov D. V. Plasma physics]. СПб: изд-во Политехнического ун-та. 2013. 542 с. DOI: 10.18720/SPBPU/2/si20-969.

Received 17.09.2023.